Section 5

Development of and studies with regional and smaller-scale atmospheric models, regional ensemble, monthly and seasonal forecasting

Intercomparison of Spatial Verification Methods for COSMO Terrain (INSPECT): Preliminary Results

Alferov D.[1], Astakhova E.[1], Boukouvala D.[2], Bundel A.[1], Damrath U.[3], Eckert P.[4], Gofa F.[2], Kirsanov A.[1], Lapillonne X.[4], Linkowska J.[5], Marsigli C.[6], Montani A.[6], Muraviev A.[1], Oberto E.[7], Tesini M.S.[6], Vela N.[7], Wyszogrodzki A.[5], Zaichenko M.[1]

(1) RHM, (2) HNMS,(3) DWD, (4) MCH,(5) IMGW-PIB, (6) ARPA-SIMC, (7) ARPA-PT

a.bundel@gmail.com

A COSMO consortium project devoted to spatial verification methods (INSPECT) has been created to follow MesoVICT activities (http://www.ral.ucar.edu/projects/icp/) and to summarize the COSMO experience of applying spatial verification methods to high and very high resolution forecast systems (deterministic and EPS). The project started in April 2015; it is planned for two years. One of the scopes of INSPECT is to propose guidelines for application of new spatial methods based on the analysis of data gained during the project.

The ICP and MesoVICT projects have already provided the setup of experiments and a set of test cases including high-resolution observations. Several INSPECT tasks involve reruns of COSMO very-high-resolution models for MesoVICT test cases with a focus on the MesoVICT core experiment and case 1. Additional periods/models will be utilized in INSPECT, e.g., the dataset of FROST-2014 project (Forecast and research in the Olympic Sochi testbed, http://frost2014.meteoinfo.ru/). The FROST models provide longer timeseries compared to MesoVICT test cases. The Sochi data focuses on winter season, which is very important for the mountainous regions. It will be useful to carry out comparison for two complex terrains: the Alps and the Caucasus with their peculiar features. The COSMO versions will be compared with other models, which is highly beneficial for improvements of models.

Until now, COSMO studies on spatial verification methods have been concentrated mainly on the deterministic precipitation field representation and the useful scales of high- or very-high-resolution models. One of the main aims of INSPECT is to investigate the additional information gained by the application of such methods to other fields such as wind speed, as well as the possibility to apply spatial verification methods to COSMO ensemble forecast systems, such as the COSMO-LEPS.

Almost all groups of methods are involved in INSPECT: in the first place, the most popular neighborhood-based approaches (summarized in Ebert, 2008); features-based approaches (Contiguous Rain Area (CRA) (Ebert and McBride, 2000), method for Object-based Diagnostic Evaluation (MODE) tool (Davis et al., 2006), SAL technique (Wernli et al., 2008)); and scale decomposition. Also, the DIST method developed at ARPA-SIMC (Marsigli, C. et al., 2008) will be studied; the DIST method is a kind of upscaling methods.

Special attention will be given to the verification strategy for analyzing extreme weather events, utilizing the intense precipitation cases that are included in MesoVICT experiments. It will be studied if spatial verification techniques can be successfully used in such cases and if such scores as the EDI, SEDI can be applied to upscaled data.

The R SpatialVx, COSMO VAST package, and IDL Beth Ebert's tool will be used to run the spatial methods.

The first results obtained concern applications at DWD, where the FSS and ETS for the upscaling method are calculated for 6-hr precipitation data over the entire German territory since 2007, providing plots of long-term trend of these indices. It is shown that a lower threshold and larger window give the highest skill. Such plots allow compact representation of the neighborhood scores (Fig. 1).

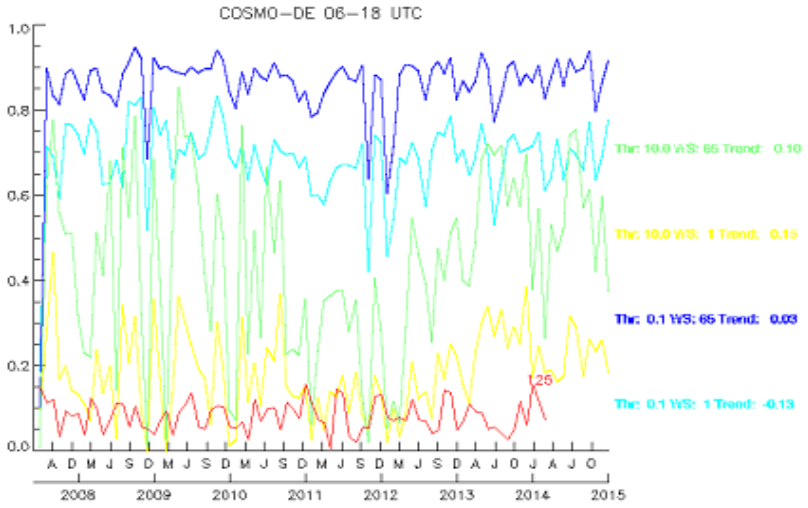

Fig. 1. Time series of the fraction skill score over the whole German territory, COSMO-DE model with 2.8 km resolution, 6h precipitation accumulations (06-18h UTC), for two precipitation thresholds (> 0.1 mm/6h and > 10.0 mm/6h) and two windows (1 and 65 boxes)

References:

1. Davis, C., B. Brown, and R. Bullock, 2006: Object-based verification of precipitation forecasts. Part I: Methodology and application to mesoscale rain areas. Mon. Wea. Rev., 134, 1772–1784.
2. Ebert, E. and J. McBride, 2000: Verification of precipitation in weather systems: Determination of systematic errors. J. Hydrol., 239,179–202.
3. Ebert, E., 2008: Fuzzy verification of high resolution gridded forecasts: A review and proposed framework. Meteor. Appl., 15, 51–64, doi:10.1002/met.25.
4. Marsigli, C., Montani, A. and Paccangnella, T. (2008), A spatial verification method applied to the evaluation of high-resolution ensemble forecasts. Met. Apps, 15: 125–143. doi: 10.1002/met.65
5. Wernli , H., M. Paulat, M. Hagen and C. Frei, 2008: SAL - a novel quality measure for the verification of quantitative precipitation forecasts. Mon. Wea. Rev., 136, 4470-4487

A new operational regional model for convection-permitting numerical weather prediction at JMA

KOHEI ARANAMI, TABITO HARA, YASUTAKA IKUTA, KOHEI KAWANO, KENGO MATSUBAYASHI, HIROSHI KUSABIRAKI, TAKAHIRO ITO, TAKUMU EGAWA, KOJI YAMASHITA, YUKINARI OTA, YOSHIHIRO ISHIKAWA, TADASHI FUJITA, AND JUN-ICHI ISHIDA

Numerical Prediction Division, Japan Meteorological Agency
1-3-4, Otemachi, Chiyoda-ku, Tokyo 100-8122, Japan

1 Introduction

In January 2015, a new model developed by the Japan Meteorological Agency (JMA) was put into operation in JMA's convection-permitting regional NWP system LFM (Hara et al. 2013). It replaced the previous system based on the JMA-NHM. Three new components were introduced into LFM – a new dynamical core "ASUCA" (Ishida et al. 2009, 2010), a physical processes package "the Physics Library" (Hara et al. 2012), and a variational data assimilation system "ASUCA-Var" (Fujita et al. 2013). The LFM is a very short-range numerical weather prediction system with a horizontal grid spacing of 2 km. One of its main purposes is to provide quantitative precipitation forecasts (QPFs) for disaster prevention information. It was confirmed that the LFM based on ASUCA (referred to here as the ASUCA-LFM) has a similar level of statistical performance in terms of QPF to the LFM based on the JMA-NHM (referred to here as the NHM-LFM).

This report outlines differences between the ASUCA-LFM and the NHM-LFM, with focus on improvements made to physical processes, data-assimilation system and optimisation, as well as the results of a performance evaluation experiment conducted with the same configuration as the previous operational model.

2 Major updates from the NHM-LFM to the ASUCA-LFM

2.1 Dynamics updates

As described in Ishida et al. (2009, 2010), most of the dynamics were upgraded (e.g., finite volume vs. finite difference, RK3 vs. leap-frog, flux limiter vs. flux correction, time-splitting treatment of precipitable water), which enables the use of a longer time-step interval (16.67 sec vs. 8 sec) without computational instability.

2.2 Physics updates

As described in Hara et al. (2012), physical processes available in the ASUCA-LFM are at least equivalent to those of the NHM-LFM. In fact, numerous improvements are already included in the Physics Library, such as the boundary layer scheme related to the computational stability (Hara 2010), implicit coupling of boundary layer scheme and surface flux scheme, surface flux tiling (i.e., the capacity for consideration of land/sea sub-grid effects in a grid), and the parameterization for convective initiations (Hara 2015). These improvements have been readily incorporated into ASUCA as demonstrated in Hara et al. (2012), resulting in better forecast performance in certain areas as outlined below.

2.3 Optimisation

One of the original motivations in the development of a new dynamical core was the achievement of better computational efficiency on scalar multi-core architecture. Although not described in detail here, the ASUCA-LFM involves a number of computationally expensive factors (e.g., implicit discretization in physics, absence of spatial density reduction in radiation, RK3 instead of the forward-backward for sound wave treatment, and doubling of the I/O size). As a consequence, it was found that the computational expense of the ASUCA-LFM in terms of FLOP is 1.2 times greater than that of the NHM-LFM. However, due to more efficient cache usage, overlapping of communication and computation, and offloading of I/O using io-servers, the ASUCA-LFM completes computation of a nine-hour forecast slightly faster than the NHM-LFM.

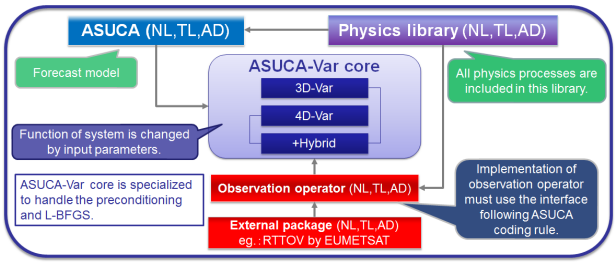

Fig. 1: Schematic diagram of ASUCA, Physics Library, and ASUCA-Var.

2.4 ASUCA-Var

One of the major upgrades to the system is the adoption of ASUCA-Var – a variational data assimilation system based on ASUCA. Fig. 1 shows a schematic diagram of the new framework (ASUCA, Physics Library and ASUCA-Var), in which non-linear (NL), tangent-linear (TL) and adjoint (AD) models are developed in an organised and coordinated way (e.g., TL, NL and AD are included in the same file). This schematic illustrates the ultimate goal of the framework, which is as yet incomplete, and the 3D-Var part of the framework has been incorporated into the ASUCA-LFM. In ASUCA-Var, the forward operators (e.g., observation operator) are TL, whilst JNoVA, which is a 3D-Var system based on the JMA-NHM, employs NL operators. Soil temperature and soil moisture have also been introduced as control variables. Background error was also improved; this was set uniformly in space in JNoVA, but can be set for individual grids in ASUCA-Var. This means, for example, that increment over land can be prevented from spreading over sea areas. Two-dimensional decomposition is also implemented in ASUCA-Var. Atmospheric motion vectors (AMVs) have been additionally incorporated for satellite data.

3 Performance evaluation experiment

An experiment was carried out to evaluate the performance of the ASUCA-LFM as an operational convection-permitting model. The experimental period covered 40 days in each of winter and summer, initialised at three hourly (i.e., 240 initials each). Fig. 2 and Fig. 3 show the equitable threat score (ETS) and the bias score(BS) for the winter and summer periods, respectively. It can be seen that levels of QPF accuracy for the two periods are statistically similar.

*E-mail: aranami@met.kishou.go.jp

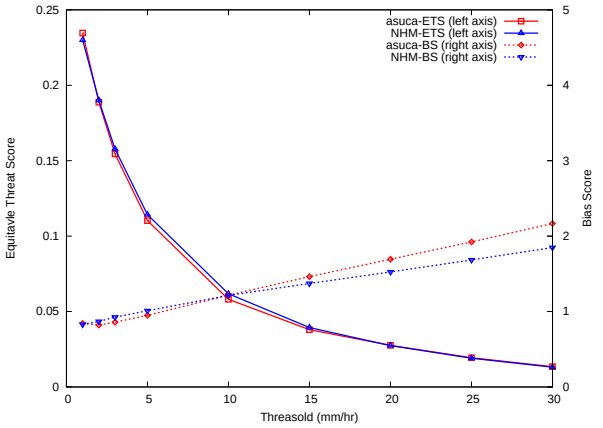

Fig. 2: Equitable threat score (solid lines, left axis) and bias score (dashed lines, right axes) for the summer experiment. Red lines indicate the scores of ASUCA-LFM, and the blue lines indicate the score of NHM-LFM. x-axis indicates threshold in mm/hr.

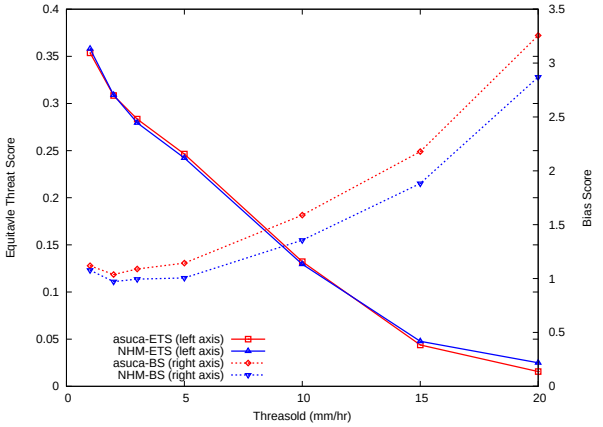

Fig. 3: Same as Fig. 2 but for the winter experiment.

Although the precipitation forecasts have similar overall accuracy, some aspects are better with the ASUCA-LFM. One such improvement is the enhanced representation of the diurnal cycle of rainfall consisting of showers associated with unstably stratified layers. The introduction of the parameterization for convective initiation (Hara 2015) is a primary factor behind this improvement.

It was also confirmed that forecast performance for near-surface variables (including 10-m wind, screen level temperature and humidity) is statistically similar or better. One exception is surface pressure, where forecasting was less accurate due to the exact mass conservation of the ASUCA-LFM. That is, the ASUCA-LFM represents the total mass change of the coarser model (which provides the lateral boundary conditions for LFM) better than the NHM-LFM.

Fig. 4 shows observed and simulated infrared images of a cold-air outbreak case in the winter experiment. It can be seen that ASUCA-LFM produces more realistic (low-level) cloud associated with this cold air than the NHM-LFM. It was also found that these differences can be generally seen for instances of cold air outbreak, mainly due to the improvement of the boundary layers scheme.

4 Conclusions

The new operational-limited area model based on ASUCA, the Physics Library, and ASUCA-Var was successfully launched in January 2015. This represents only the start of development based on these components rather than being a goal in itself. In future work, ASUCA will be introduced for another coarser regional model (known as the Meso-Scale Model) at JMA with a horizontal grid spacing of 5 km and a longer forecast period. As indicated by Hara et al. (2012), the Physics Library provides a basis of the "seamless" developments, which is highly important for further progress in the field.

References

Fujita, T., Y. Ishikawa, Y. Ikuta, K. Ono, K. Ishii, K. Yoshimoto, J. Ishida, T. Hara, K. Kawano, H. Kurahashi, K. Matsubayashi, N. Kinoshita, T. Egawa, Y. Kosaka, and H. Eito, 2013: Development of the Operational Data Assymilation System for Rapid Frequent Updates of Forecast with the Convection-Permitting Model at JMA. *WMO Sixth Symposium on Data Assimilation.*

Hara, T., 2010: Comparisons on the boundary layer schemes using a single column model. *Proceedings of the First International Workshop on Nonhydrostatic Numerical Models*, **1**, 19–20.

Hara, T., 2015: Necessity of parameterizations for convective initiations in high resolution cloud permitting models. *CAS/JSC WGNE Research Activities in Atmospheric and Oceanic Modelling.*, **45**, submitted.

Hara, T., K. Kawano, K. Aranami, Y. Kitamura, M. Sakamoto, H. Kusabiraki, C. Muroi, and J. Ishida, 2012: Development of Physics Library and its application to ASUCA. *CAS/JSC WGNE Research Activities in Atmospheric and Oceanic Modelling.*, **42**, 0505–0506.

Hara, T., T. Fujita, S. Moriyasu, K. Kawano, Y. Ikuta, Y. Hayashi, K. Matsubayashi, N. Kinoshita, and H. Eito, 2013: The operational convection-permitting regional model at JMA. *CAS/JSC WGNE Research Activities in Atmospheric and Oceanic Modelling.*, **43**, 0505–0506.

Ishida, J., C. Muroi, and Y. Aikawa, 2009: Development of a new dynamical core for the nonhydrostatic model. *CAS/JSC WGNE Research Activities in Atmospheric and Oceanic Modelling.*, **39**, 0509–0510.

Ishida, J., C. Muroi, K. Kawano, and Y. Kitamura, 2010: Development of a new nonhydrostatic model "ASUCA" at JMA. *CAS/JSC WGNE Research Activities in Atmospheric and Oceanic Modelling.*, **40**, 0511–0512.

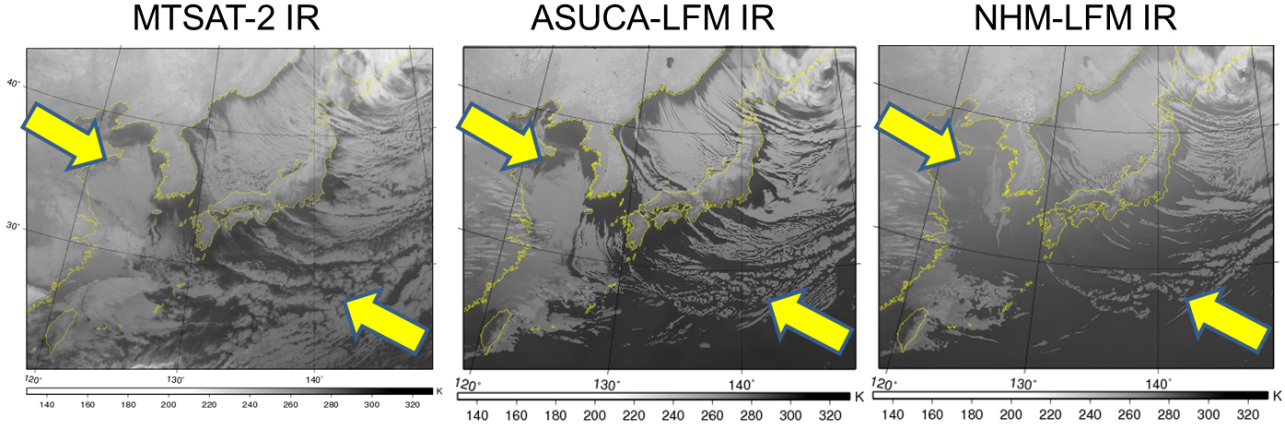

Fig. 4: Observed infra-red satellite image (left), simulated image using ASUCA-LFM (centre) and NHM-LFM (right) for a case of cold air outbreak.

Findings from temporal nudging experiments of sea surface temperature

Hae-Cheol Kim[1,*], Carlos Lozano[2], Dan Iredell[1], Hyun-Sook Kim[1], Avichal Mehra[2], Liyan Liu[1]
[1] IMSG at NWS/NCEP/EMC, [2] NWS/NCEP/EMC
Email: Hae-Cheol.Kim@noaa.gov

The ocean states represented in the ocean model component in a coupled atmosphere-ocean hurricane forecast system are required to maintain an accurate representation of the upper ocean and major mesoscale features, in particular, during the hurricane season along the hurricane paths. In support of this requirement this study examines some aspects of data assimilation in a regional ocean model for the Western North Atlantic (HAT11W) to be used as an ocean component of an operational coupled atmosphere-ocean hurricane forecast system, the Hurricane Weather Research Forecast-Hybrid Coordinate Ocean Model (HWRF-HYCOM). Specifically, a series of numerical experiments are conducted for the period that covers normal and hurricane-intensity conditions during Hurricane Isaac (Aug. 21 – Sep 1, 2012) which was a destructive hurricane that came ashore in the U.S. state of Louisiana during August 2012. Various nudging scales of sea surface temperature (SST) are examined to explore the appropriate temporal range of nudging SST in a regionally nested domain (HAT11W). These SST fields are from the Global Real-Time Ocean Forecast System (RTOFS-Global [1]; http://polar.ncep.noaa.gov/global/) which is an operational ocean weather forecast system at the National Centers for Environmental Prediction (NCEP), National Weather Service (NWS).

HAT11W is nested as a sub-domain within RTOFS-Global with its boundary conditions defined from the outer global domain. The numerical ocean modeling component is the eddy-resolving $1/12^{o}$ HYbrid Coordinate Ocean Model (HYCOM) with horizontal recti-linear coordinate. Vertical coordinates employ 32 layers, following isopycnals in the deep sea, z-levels in the surface and a terrain-following σ-coordinate near coastal areas [2]. K-Profile Parameterization (KPP) [3] is used as a vertical mixing scheme. RTOFS-global is re-initialized every day from an analysis prepared by the Naval Oceanographic Office (NAVOCEANO) using a multivariate optimal interpolation (MVOI) scheme [4] for assimilating observations collected from various platforms. In this study, we focus on the simplest configuration in which we can isolate the effects of the global model fields with atmospheric forcings from NCEP's Global Data Analysis System (GDAS) and Global Forecast System (GFS), in order to understand the pure effect of driving the SST fields of the model at the surface with an SST analysis based on observations. The analysis employed in this study ingests SST observations derived from the Advanced Very High Resolution Radiometer (AVHRR).

The updated SST field is based on a two-dimensional variational (2DVAR) analysis [5]. Time interpolated SST analysis fields are included in the temperature tendency of the surface layer by nudging with a relaxation time scale (rlxsst). The additional heat flux added to the surface is distributed by vertical mixing, horizontal advection and eddy diffusivity with the main physical process distributing the additional heat flux being vertical turbulence. The intent of nudging at the surface is to gently steer the mixed layer (ML) temperature toward observations.

A comparison of ML averaged temperature between the free (Expt000) and a strong nudging case (Expt007) is done for Sep. 3, 2012, 00Z, after 50 days of initialization (Fig.1). Compared to the free run, the distribution of ML averaged temperature is noticeably different in the assimilated fields. For example, temperature patterns in the Gulf of Mexico tend to be warmer offshore but colder in the coastal areas in data assimilative mode. Overall, this tendency is true for the Caribbean region as well. Cold water mass along the South American coast (Venezuela to Brazil) presented in Expt000 disappeared in Expt007. In addition, warm/cold patches of Expt000 have been diffused in Expt007 when SST observations are assimilated, which is as anticipated.

Some of our findings are highlighted in Figure 2. A nudging scale (rlxsst) of 1 day (the black line in Fig. 2) yields the minimum root mean square error (RMSE) of innovation, but it injects large negative heat fluxes (approximately -1.38 KWm^{-2} for ΔT=1 °C) onto the surface leading to rapid entrainment (artificial negative buoyancy), which is not expected in this region. This can be avoided by limiting the

change in heat flux (>-1KWm^{-2}). In our experiments, the implicit KPP algorithm converges with four iterations under both normal/abnormal conditions away from hurricane footprint with/without SST nudging. Without limiting the size of assimilated fluxes we find that the nudging scale of 6 days is the optimum time scale for SST nudging in the upper ocean in our region of study. For general circulation patterns, after 50-day simulations RTOFS-Global and those experiments with appropriate nudging scales were similar. This suggests that six day forecasts will give reasonable results in the absence of strong dynamical events.

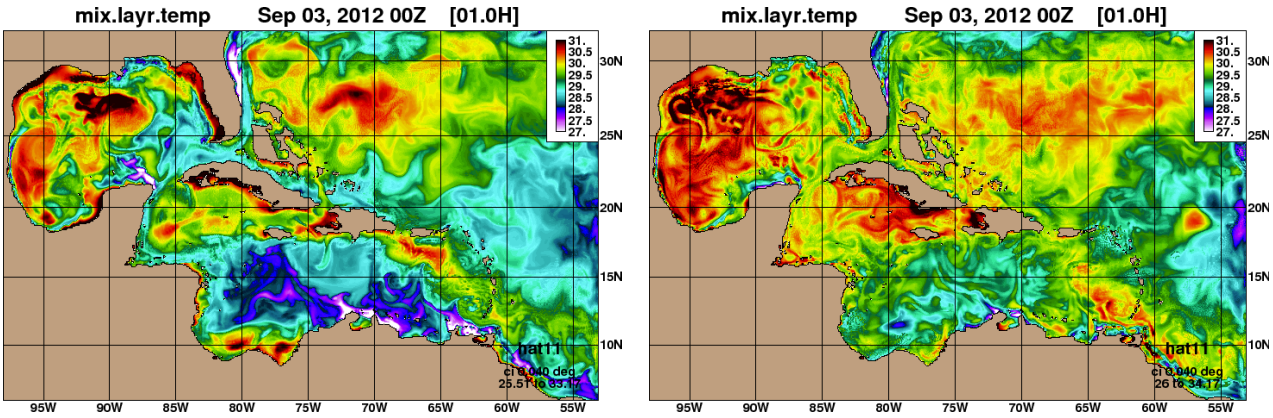

Fig. 1. Mixed layer (ML) averaged temperature fields for the same day are compared for Expt000 (left) and Expt007 (right).

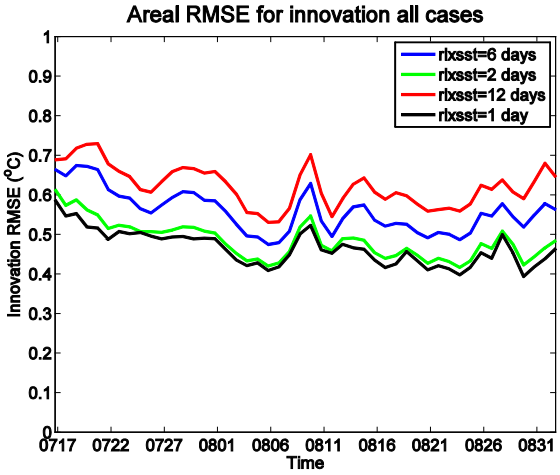

Fig. 2. Time evolution of RMSE for innovation for different settings of relaxation scale.

[1] Mehra, A., I. Rivin, H. Tolman,T. Spindler and B. Balasubramaniyan, 2011. A Real-Time operational GlobalOcean Forecast System. *GODAE OceanView - GSOP - CLIVAR Workshop on Observing System Evaluation and Intercomparisons*, Univ. of California Santa Cruz, CA, USA, 13-17 June 2011

[2] Bleck, R., 2002: An oceanic general circulation model framed in hybrid isopycnic-Cartesian coordinates, *Ocean Model.*, 37, 55-88.

[3] Large, W.C., J.C. McWilliams and S.C. Doney, 1994: Oceanic vertical ixing: a review and a model wit a nonlocal boundary layer parameterization. *Rev. Geophys.* 32, 363-403.

[4] Cummings, J. A., 2005: Operational multivariate ocean data assimilation. *Q. J. Roy. Meteor. Soc.*, 131, 3583–3604.

[5] Purser, R. J., W.-S. Wu, D. F. Parrish, and N. M. Roberts, 2003b: Numerical aspects of the application of recursive filters to variational statistical analysis. Part II: Spatially inhomogeneous and anisotropic general covariances. *Mon. Wea. Rev.*, 131, 1536—1548.

The National Air Quality Forecasting Capability

Jeff McQueen
Environmental Modeling Center
NCEP/NWS/NOAA/DOC
College Park, MD 20740
e-mail: Jeff.mcqueen@noaa.gov

The United States National Weather Service National Air Quality Forecasting Capability (NAQFC) system is an off-line coupled atmospheric chemical concentration forecasting modeling system using the National Centers for Environmental Predictions (NCEP) North American Meso-scale non-hydrostatic Model (NAM/NMMB) to drive the Environmental Protection Agency (EPA) Community Multi-scale AQ model (CMAQ) with the CB05 gaseous and AERO4 aerosol chemistry options -- run at 12 km horizontal resolution to 48 hours twice per day. CMAQ solves the material continuity equation for the chemical constituents in the troposphere. In so doing it provides forecasts for surface ozone (O3) and fine particulate matter (PM) concentrations for the nation. Chemical lateral boundary conditions for inflow are adopted from a species mapping methodology (Tang et al., 2009), matching constituents between the CMAQ with those from a global Harvard University GEOS-Chem model climatology. Tests incorporating the NWS NGAC predicted aerosols at the CMAQ lateral boundary conditions are on-going with operational implementation expected later in 2015.

The emission dataset is built on top of the 2011 National Air Quality Forecasting Capability (NAQFC) 2011 baseline data, but with four major updates: (a) new point source emissions with updated emission measurements and energy projections; (b) new mobile source emissions updated to 2012 based on a trends from the U.S. EPA surface monitoring network corroborated with satellite trends for the same constituents (Tong et al., 2015); (c) new off-road emissions projected to 2012; and (d) updated Canadian emission sectors from Environment Canada (EC) 2012 emission inventories and the Mexican 2010 National Inventory for Mexico. The NOAA Hazard Mapping System (HMS) is used to detect wild fires over the Nation. The HMS product is then used to drive the U.S. Forest Service BlueSky wild fire emissions system. Other intermittent sources are also included. Finally, A Kalman filter based bias correction scheme (Djalalova, et al. 2015) has provided improved PM prediction skill that should result in improved guidance for State environmental agencies responsible for air quality alerts.

References

Djalalova, I., L. Delle Monache., J. Wilczak (2015): PM2.5 analog forecast and Kalman filter post-processing for the Community Multiscale Air Quality (CMAQ) model, Atmospheric Environment, 108,

76-87, doi:10.1016/j.atmosenv.2015.02.021.

Tang, Y., P. Lee, M. Tsidulko, H.-C. Huang, J. T. McQueen, G. J. DiMego, L. K. Emmons, R. B.Pierce, H.-M. Lin, D. Kang, D. Tong, S. Yu, R. Mathur, J. E. Pleim, T. L. Otte, G. Pouliot, J. O. Young, K. L. Schere, P. M. Davidson, I. Stajner (2009): The Impact of Chemical Lateral Boundary Conditions on CMAQ Predictions of Tropospheric Ozone over the Continental United States, Environmental Fluid Mechanics, 9 (1), 43-58, doi:10.1007/s10652-008-9092-5.

Tong, D.Q , L. Lamsal, L. Pan, C. Ding, H-C. Kim, P. Lee, T. Chai, K. E. Pickering, I. Stajner (2015): Long-term NOx trends over large cities in the United States during the Great Recession Comparison of satellite retrievals, ground observations, and emission inventories Atmospheric Environment 01/2015; 109. DOI:10.1016/j.atmosenv.2015.01.035

Impact of high-resolution boundary conditions on the quality of COSMO-LEPS forecasts

Andrea Montani, C. Marsigli, T. Paccagnella

ARPA–SIMC, Bologna, Italy

Introduction

In the framework of the development of European LAMEPSs, the ECMWF Research Department performed a number of global-model ENS reruns at the resolution of about 16 km. Data were provided for three two-week periods (in total 46 days), selected in such a way to encompass several high-impact weather events occurred over Europe (further details under `https://software.ecmwf.int/wiki/display/LAMEPS/LAMEPS+Home`). The availability of this unique dataset made possible the performance of several tests by the LAMEPS community. As for the experimentation with COSMO–LEPS (Montani et al., 2011), the limited-area-model ensemble prediction system operationally run by ARPA-SIMC on behalf of the COSMO Consortium (`http://www.cosmo-model.org`), the attention was focused on the performance of the system driven by this high-resolution ENS experiments.

Methodology and results

Four different sets of ensembles were compared:

1. **opecleps** ($\Delta x = 7$ km, 40 Model Levels, 16 members), the operational COSMO-LEPS running at the time of the weather events (COSMO version 4.12) and nested on the operational ECMWF ENS;
2. **TESTcleps_OldModel** ($\Delta x = 7$ km, 40 Model Levels, 16 members), the test version of COSMO-LEPS nested on high-resolution ENS (COSMO version 4.12);
3. **TESTcleps_NewModel** ($\Delta x = 7$ km, 40 Model Levels, 16 members), the same as "TESTcleps_OldModel", but with COSMO version 4.26, with new microphysics;
4. **H_ENS** ($\Delta x = 16$ km, 62 Model Levels, 21 members), the high-resolution global ENS, driving both "TESTcleps" systems.

In order to compare the skill of the 4 systems, we considered the probabilistic prediction of total precipitation exceeding a number of thresholds for several forecast ranges, analysing the performance of the runs starting at 12UTC. The evaluation of the models' performances was carried out over the full COSMO-LEPS domain, covering the area [35-58N, 10W-30E]. As for observations, it was decided to use the data obtained from the SYNOP reports available on the Global Telecommunication System, about 1440 in the verification domain. The comparison of model forecasts against observations was carried out by selecting the model grid-point closest to the observation. The skill of the different systems was examined for 6 different precipitation thresholds: 1, 5, 10, 15, 25 and 50 mm/12h. The following probabilistic scores were computed: the Brier Skill Score (BSS), the Ranked Probability Skill Score (RPSS), the Relative Operating Characteristic Curve (ROC) area, the Rank Histograms (RK) and the Percentage of Outliers (OUTL). For a description of the scores, the reader is referred to Wilks (1995).

The forecast skills of COSMO ensembles and H_ENS are summarised in Fig. 1, which presents the results in terms of probabilistic prediction of 12-hour cumulated precipitation for the full length of the verification exercise. The left panel of the figure reports the values of the RPSS plotted against the forecast range. It can be noticed that very similar results are obtained by opecleps and TESTcleps_OldModel (red and green lines, respectively) for almost all forecast ranges. These two systems differ mainly on the quality of the boundaries, which are

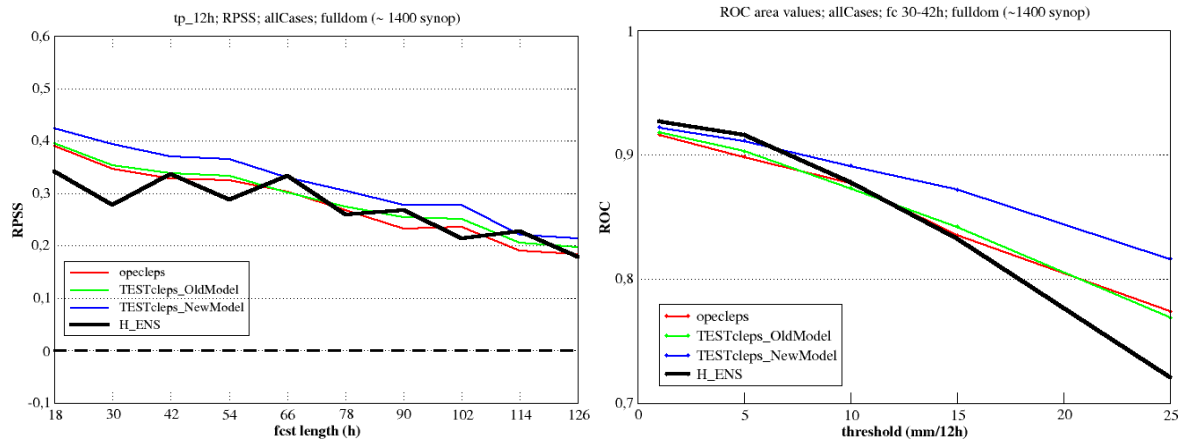

Figure 1: Verification of 12-hour cumulated precipitation: RPSS values as a function of the forecast range (left panel) and ROC area values as a function of the threshold value for the range 30-42h (right panel). Scores are reported for the following systems: opecleps (red), TESTcleps_OldModel (green), TESTcleps_NewModel (blue) and H_ENS (thick–black).

provided at higher resolution in the latter configuration. Therefore, it looks as if the benefits of more detailed boundaries are only partly transferred to the skill of the limited-area integrations. A slight positive impact can be noticed for ranges longer than 78 hours, when TESTcleps_OldModel shows higher scores than opecleps. The best results are obtained by the TESTcleps_NewModel configuration (blue line), where COSMO–LEPS benefits of both higher-resolution boundaries by H_ENS and improved model set-up. The better performance of TESTcleps_NewModel is evident for all ranges and is especially true for short forecast steps. As for the global ensemble H_ENS, it can be noticed that its performance is the worst one in the short range, while the system gets more valuable for longer ranges. The right panel of the Fig. 1 shows the ROC area values for the forecast range 30-42h as a function of precipitation intensity. The above–mentioned results are confirmed: the highest scores are obtained by TESTcleps_NewModel, with similar performances by opecleps and TESTcleps_OldModel. As for H_ENS, the performance of the model is satisfactory for low threshold events, while the system shows a performance decay for high-precipitation cases, suggesting the added value of limited–area ensemble forecasting for cases of heavy rain.
Therefore, the main results of the verification exercise carried out in the framework of LAMEPS experimentation can be summarised as follows:

- the impact of using high-resolution boundaries with respect to the operational configuration is limited;
- a clear improvement in limited-area model integrations is obtaibed if, in addition to high resolution boundaries, a newer model version with updated microphysics is used;
- in either cases, the added value with respect to the global ensemble is noticeable, especially in the short range.

As for the future, it is planned to consolidate the verification results, by considering the performance of all systems for other variables, considering also the spread/skill performance for the different periods.

References

Montani A., Cesari D., Marsigli C., Paccagnella T., 2011. Seven years of activity in the field of mesoscale ensemble forecasting by the COSMO–LEPS system: main achievements and open challenges. *Tellus*, **63A**, 605-624. DOI: 10.1111/j.1600-0870.2010.00499.x

Wilks, D.S., 1995. Statistical Methods in the Atmospheric Sciences. Academic Press, New York, 467.

Performance of the COSMO-based ensemble systems during Sochi-2014 pre-Olympics

Andrea Montani[1], D. Alferov[2], E. Astakhova[2], C. Marsigli[1], T. Paccagnella[1]

[1]*ARPA–SIMC, Bologna, Italy*

[2]*Hydrometcenter of Russia, Moscow, Russia*

Introduction

The Winter Olympics and Paralympic Games took place in Sochi, Russia, from 7 to 23 February 2014 and from 7 to 16 March 2014. In the framework of these events, WMO WWRP initiated a dedicated blended Forecast Demonstration/Research and Development Project (FDP/RDP). **FROST-2014** (**F**orecast and **R**esearch in the **O**lympic **S**ochi **T**estbed; `http://frost2014.meteoinfo.ru/`) aimed at advancing the understanding of nowcasting and short-range prediction processes over complex terrain (Kiktev, 2011). In the framework of probabilistic forecasting, the following actions were undertaken by the COSMO consortium (`http://www.cosmo-model.org`) to support NWP aspects of FROST-2014:

(1) FDP part: relocation of COSMO-LEPS (Montani et al., 2011) over the Sochi area, generating a new system named COSMO-S14-EPS ("S14" stands for Sochi2014);
(2) RDP part: development of a convective-scale ensemble system for the Sochi area, referred to as COSMO-Ru2-EPS ("Ru2" stands for Russian 2.2 km).

As for (1), COSMO-S14-EPS, the convection-parameterized ensemble prediction system based on COSMO model and targeted for the Sochi-area, was implemented on ECMWF super–computers and ran on a regular basis from 19 December 2011 to 30 April 2014. The forecast fields were used to generate a set of standard probabilistic products, including probability of surpassing a threshold, ensemble mean and ensemble standard-deviation for several surface and upper-air variables. The individual forecast members were also transferred to the Hydrometcenter of Russia, where the epsgrams for predetermined points (mainly, locations of outdoor and indoor competitions) were prepared. All these products were used in real time by the Sochi forecasters via the FROST-2014 Web-site (`http://frost2014.meteoinfo.ru/forecast/goomap` and `http://frost2014.meteoinfo.ru/forecast/arpa-new/`). In addition to the probabilistic guidance for the prediction of high–impact weather over the Olympic areas up to day 3, COSMO-S14-EPS provided initial and boundary conditions for activity (2), linked to the generation of the convective-permitting ensemble COSMO-Ru2-EPS, which ran in Moscow on a quasi-operational basis between January and February 2013 as well as from November 2013 to April 2014. Table 1 summarises the main features of both systems.

Table 1: Main characteristics of COSMO-S14-EPS and COSMO-Ru2-EPS.

	COSMO-S14-EPS	COSMO-Ru2-EPS
Horizontal/vertical resolution	7 km /40 ML	2.2 km / 50 ML
Forecast length	72h	48h
Ensemble size	10	10
Initial time	00/12 UTC	00/12 UTC
Convection	Parameterized	Resolved

Verification results

The skills of COSMO-S14-EPS and COSMO-Ru2-EPS are assessed over the period January-February 2013. For both systems, we considered the probabilistic prediction of 2-metre temperature exceeding a number of thresholds for several forecast ranges. As for observations, the data obtained from the SYNOP reports available on the Global Telecommunication System

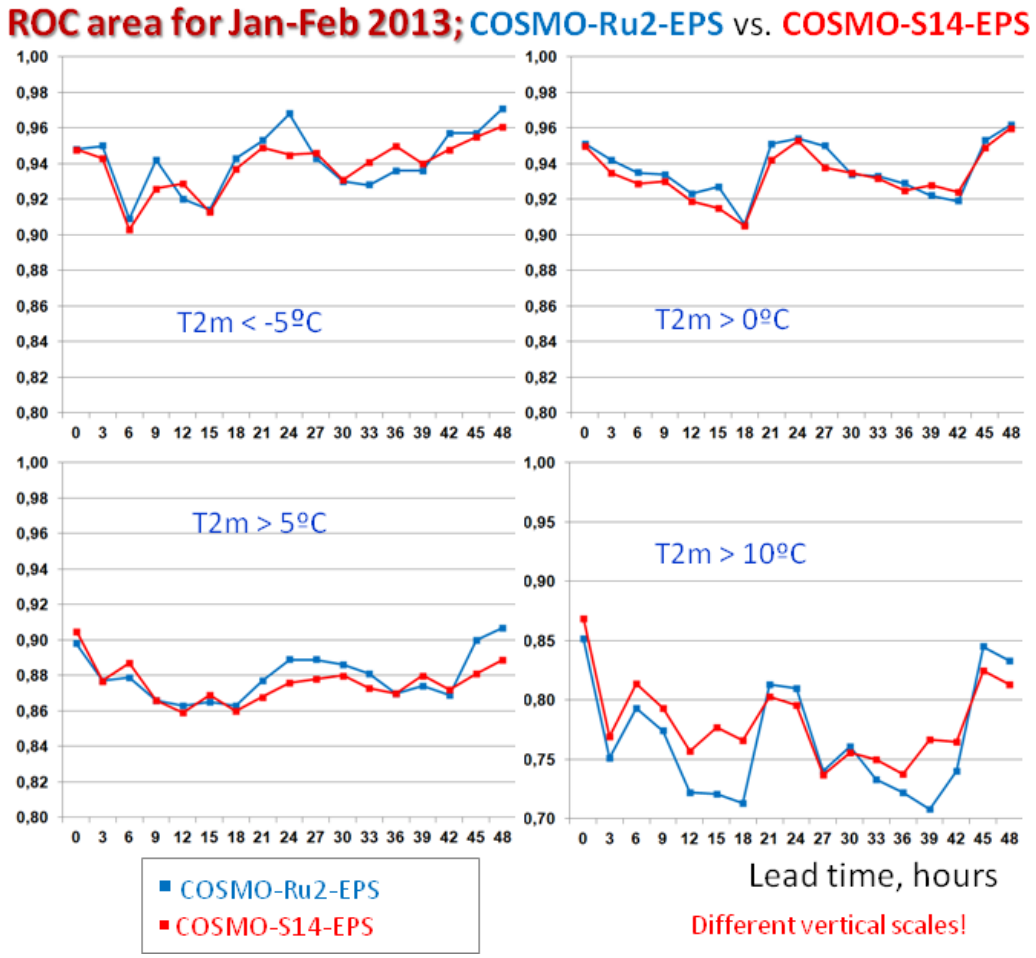

Figure 1: ROC area values as a function of forecast range for four different weather events: T2M below -5^{o}C (top-left panel), above 0^{o}C (top right), above +5^{o}C (bottom left) and above +10^{o}C (bottom-right with different vertical scales). The scores are calculated over the period January-February 2013. Red (blue) lines refer to COSMO-S14-EPS (COSMO-Ru2-EPS).

(GTS) as well as from a number of non-GTS local stations were used in an area centred on the Olympic venue (42.5-45N, 37.5-41.5E). The performance was examined for 4 different thresholds: -5, 0, +5 and +10 ^{o}C. The skill of two systems in terms of probabilistic prediction of 2-metre temperature is summarised in Fig. 1, where the values of the Relative Operating Characteristic (ROC) area are plotted against the forecast range for the above-mentioned weather events. The ROC area values are well above 0.8 for three out of the four thresholds, indicating that both COSMO-S14-EPS and COSMO-Ru2-EPS manage to discriminate these events. The performance of two systems is quite similar, with a slight predominance of COSMO-Ru2-EPS which has higher scores for most of the thresholds/forecast ranges. Worse scores are obtained by both systems for the highest threshold (bottom-right panel), where COSMO-S14-EPS outperforms COSMO-Ru2-EPS. It is worth pointing out that this is the rarest event with few observations; therefore, the statistical significance of this result needs to be confirmed by a more detailed investigation over a longer verification period.

References

Kiktev D., 2011. Forecast and Research: the Olympic Sochi Testbed (FROST-2014). Concept paper. Available at http://frost2014.meteoinfo.ru

Montani A., Cesari D., Marsigli C., Paccagnella T., 2011. Seven years of activity in the field of mesoscale ensemble forecasting by the COSMO-LEPS system: main achievements and open challenges. *Tellus*, **63A**, 605-624. DOI: 10.1111/j.1600-0870.2010.00499.x

Super high-resolution experiment using the JMA-NHM and the K computer

Tsutao OIZUMI[1,2], Thoru KURODA[1,2], Kazuo SAITO[2,1], Junshi Ito[2]

[1] Japan Agency for Marine-Earth Science and Technology, [2]Meteorological Research Institute

1. Introduction

In Japan, localized torrential rainfalls cause severe disasters every year. For example, debris flow in the “Izu Ohshima” island on October 15-16, 2013 has been recognized as one of the most devastating disasters in recent years. There are two observatories in the island, one is in the northern part and another is in the midwestern part near the debris flow area. The distance between two observatories is only about 4 km. However, the hourly rainfalls at the peak period (at 0300 JST, October 16) in the observatories were quite different. The hourly rainfall was 118 mm in the midwest part and 63 mm in the north part. To predict this kind of a localized torrential rainfall, a super high-resolution (several hundred meter scales) model is necessary. Many previous researchers carried out numerical experiments with higher resolutions for tornado, typhoon and heavy rain events with limited nested domains. In this study, we performed a super-high resolution (500 m) numerical weather simulation over a large domain covering thousands of km to reproduce the localized torrential rainfall using the huge computational resource of the K computer.

2. Experimental design

The case study of this research was on the Izu Ohshima heavy rainfall event on October 15-16, 2013. This study employed the Japan Meteorological Agency Non-Hydrostatic Model (NHM) and the K supercomputer. The computational domain was the same as in the previous Local Forecast Model of JMA (Figure 1) with a size of 1600 km x 1100 km. The location of Izu Oshima is indicated by a red square in Fig. 1. Table 1 shows the NHM model settings for the high resolution experiment. Initial and boundary conditions were given by the JMA Meso-scale analysis.

3. Results

We performed two experiments, with a super high resolution (HIGH: the horizontal resolution 500m) and with a low resolution (LOW: the horizontal resolution 2 km). Figure 2 shows six hour rainfall by the JMA’s precipitation analysis. Izu Ohsima was in the center of an intense rain band. Figure 3 shows observation and simulation results for one hour rainfall. In the LOW experiment, the strong rain band was simulated in the west of Izu Ohsima, and intense rain appeared in the north of the island at 0400 JST. In the HIGH experiment, the island was covered by the intense rainfall band and the strongest rainfall appeared over the area where the debris flow occurred (midwestern part of the island). The HIGH experiment captured characteristics of observed rain better than the LOW experiment. Figure 4 shows the impact of turbulence closure model on the position of the rain band. The results showed that the Deardorff scheme reduced the deviation of the rain band position in both LOW and HIGH experiments.

These results show that high resolution is important for accurate simulation of heavy rainfall. More detailed experiments are underway to see the impact of higher resolution and model domain.

Table 1. The experimental conditions. NHM parameters were selected according to model resolutions.

Horizontal resolution	Time Step (second)	NX	NY	NZ	Turbulence closure model
2 km	10	800	550	60	Mellor-Yamada level3
500 m	2	3197	2197	85	Deardorff
250 m	1	6393	4393	168	

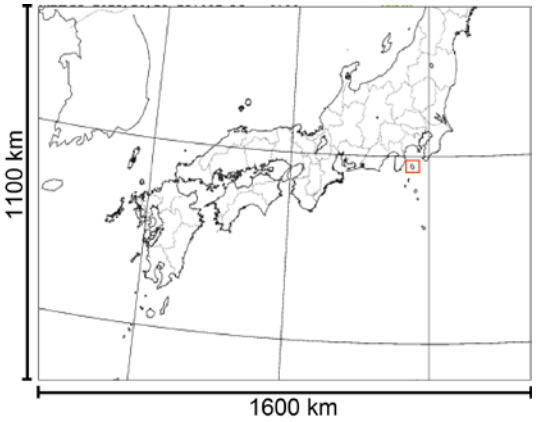

Fig. 1. Experimental domain: same as for the previous Local Forecast Model of JMA. Izu Oshima is indicated by a red square.

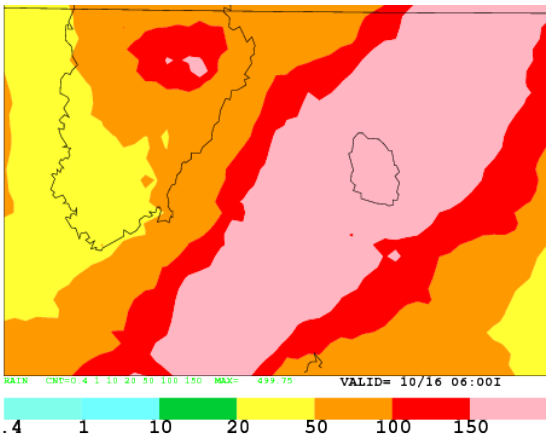

Fig. 2. Observed six-hour rainfall (until 10/16 0600 JST). The most intense 456 mm rainfall was observed in the midwestern part of the island.

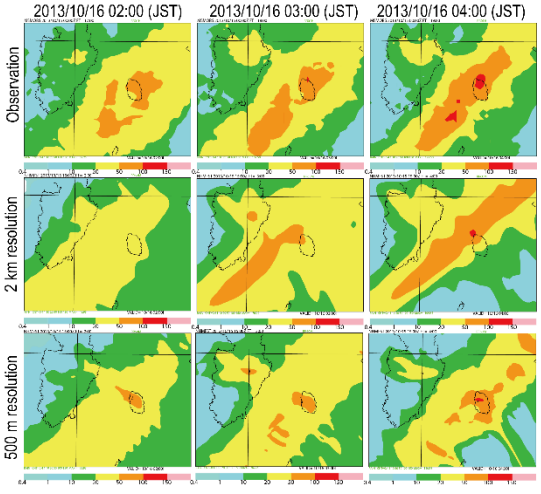

Fig. 3. Hourly rainfall from 0200 to 0400 JST by observation (upper), the HIGH experiment (middle) and the LOW experiment (bottom).

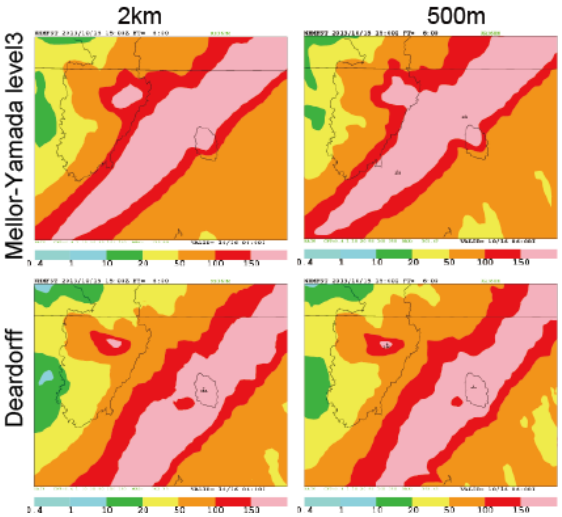

Fig. 4. Six-hour rainfall (until 10/16 0600 JST) of the HIGH and LOW experiments using the Mellor-Yamada and the Deardoff scheme.

Acknowledgments: This research used computational resources of the K computer provided by the RIKEN Advanced Institute for Computational Science through the HPCI Strategic Program for Innovation Research (Project ID:hp140220)

The Wind Features associated with the Multiple Eyewall in Typhoon Bolaven

Seiji ORIGUCHI, Kazuo SAITO, Hiromu SEKO, Wataru Mashiko and Masaru KUNII
Meteorological Research Institute, Tsukuba, Ibaraki, 305-0052,
JAPAN E-mail: origuchi@mri-jma.go.jp

1. Introduction

Typhoon 'Bolaven' passed the Okinawa Main Island at about 1200 UTC 26 August 2012, while moving northwestward. The surface observation data at Nago of Okinawa show that the rainfall intensity and surface wind speed in the typhoon's central regions were smaller and weaker than those of the JMA's operational forecast. Okinawa Meteorological Observatory held an unprecedented press conference before the approach of typhoon 'Bolaven' to take the greatest precautions for the local governments and inhabitants. However, severe damages did not actually occur. The radar images of Japan Meteorological Agency (JMA) show that the multiple eyewall structures of 'Bolaven' were clearly maintained for more than at least 24 hours without eyewall replacements. It is deduced that the structures of multiple eyewall affected the wind velocity and precipitation in the typhoon's central region. In this study, the multiple eyewall structures and wind features were reproduced by the cloud-resolving ensemble simulation to investigate the relation between them.

2. Experimental settings and Multi-Eye Index

A cloud resolving ensemble simulation with a horizontal resolution of 1 km, horizontal grids of 800×800, 60 vertical layers and 11 members was performed up to the forecast time (FT) of 24 hours from the initial time at 1800 UTC 25 August using the JMA nonhydrostatic model. The initial and boundary conditions for the cloud resolving ensemble simulation were taken from a mesoscale ensemble simulation with a horizontal resolution of 5 km. Although the triple eyewall structure was not reproduced, the typhoons with a double eyewall structure or with a single eyewall and spiral rainbands were reproduced in all members. To evaluate the degree of multiple eyewall structure objectively, the Multi-Eye Index (MEI), which indicates concentric uniformity of multiple eyewalls, was defined by formula (1):

$$\mathrm{MEI} = \frac{1}{M}\sqrt{\frac{1}{N}\sum_{i=1}^{N}(Tw_i - M)^2} \quad \left(M = \frac{1}{N}\sum_{i=1}^{N} Tw_i\right), \quad (1)$$

where *Tw* are the total water substances (cloud water, rain, cloud ice, snow, graupel) within the ring area. *N* and *M* are the number of grid points in the ring area and the average of *Tw*, respectively. The outer edge radius of the ring area corresponds to that of the outer eyewall if the typhoon has the double eyewall structure. It shows a point of the maximum tangential wind velocity on the surface. In this study, the bottom and top heights and the width of the ring area from the outer edge radius were set to be 0.5 km, 4.0 km and 2.0 km, respectively. Because MEI is sensitive to the precision of the typhoon's central position, the geometric central position estimated by the Braun's method (Braun 2002) was used as the typhoon center.

3. Experimental results and analyses

Table 1 indicates the MEIs of each member at FT=04. When MEI is 0.8 or less, it is considered that double eyewall structure was produced. In concrete terms, the typhoon of P05 had a double

eyewall structure while a spiral rainband extended from a single eyewall in M01. P05 and M01 had the lowest and highest MEI values, corresponding to the highest and lowest degrees of multiple eyewall structures, respectively.

Table 1: Multiple-Eye Index (MEI) of each member at FT=04.

Multiple-Eye structure

Spiral structure

Member	Radius of local maximum tangential velocity (km)	MEI
P05	133.0	0.58
P01	120.0	0.64
CNTL	140.0	0.69
P03	148.0	0.76
M05	134.0	0.79
M03	139.0	0.83
M02	114.0	0.89
P04	135.0	0.91
M04	124.0	0.96
P02	140.0	1.08
M01	132.0	1.17

Next, the relations between the degree of multiple eyewall structure MEI and the wind velocities are confirmed by using all ensemble members. Specifically, the correlations between MEI and the average of top 5% maximum wind of wind velocity, tangential wind velocity and radial wind velocity within 60 km radius from the typhoon center were statistically analyzed by changing the altitude at FT=04. FT=04 was selected for analysis because the multiple eyewall structures were well reproduced in a number of ensemble members at FT=04. Below the altitude of 1 km, correlations between MEI and wind velocity (tangential and inward wind velocities) were larger than 0.5 (not shown). The positive strongest correlations were shown with wind velocity and tangential wind velocity at the altitude of 0.8 km (Fig. 1). The correlations between MEI and wind velocity (tangential and inward wind velocities) below the altitude of 1 km were significantly indicated by the test of correlation coefficient (α = 5%). These results suggest that the strong winds near the surface in the central region tend to be suppressed statistically as the degrees of multiple eyewall structure are larger.

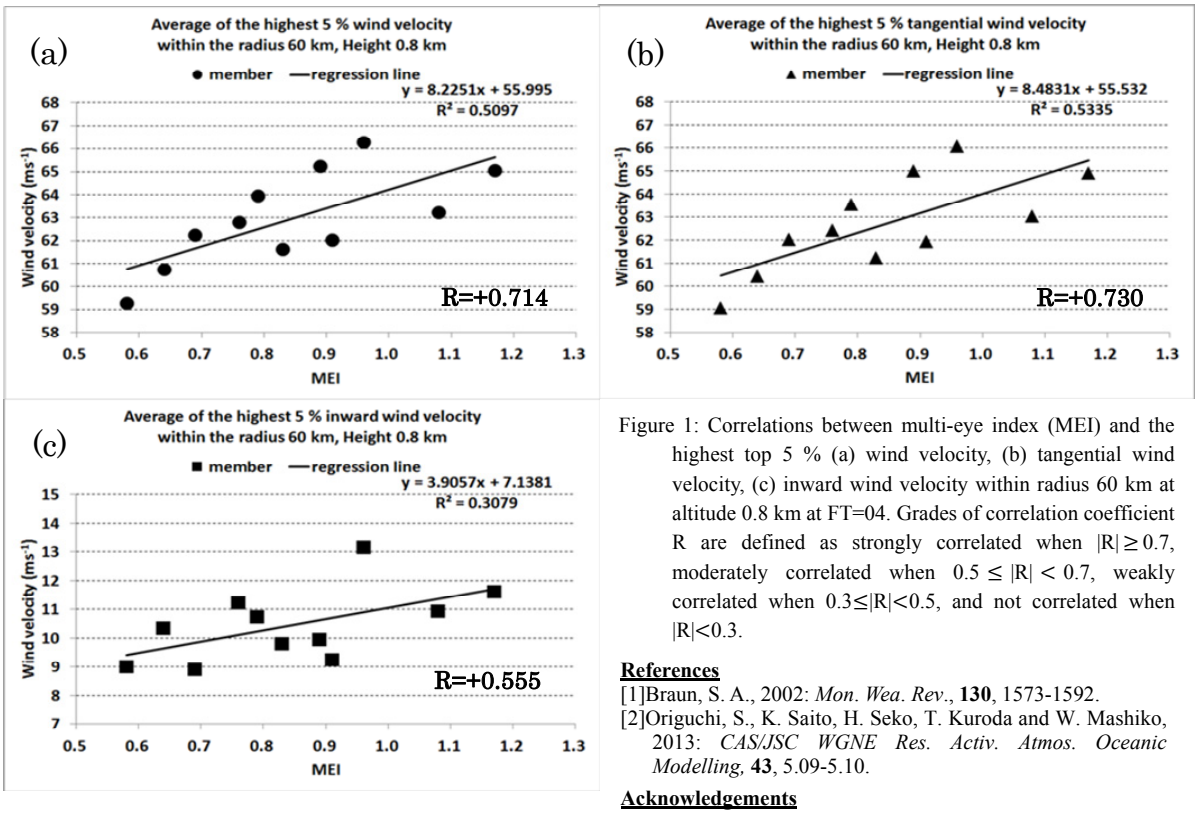

Figure 1: Correlations between multi-eye index (MEI) and the highest top 5 % (a) wind velocity, (b) tangential wind velocity, (c) inward wind velocity within radius 60 km at altitude 0.8 km at FT=04. Grades of correlation coefficient R are defined as strongly correlated when $|R| \geq 0.7$, moderately correlated when $0.5 \leq |R| < 0.7$, weakly correlated when $0.3 \leq |R| < 0.5$, and not correlated when $|R| < 0.3$.

References

[1]Braun, S. A., 2002: *Mon. Wea. Rev.*, **130**, 1573-1592.

[2]Origuchi, S., K. Saito, H. Seko, T. Kuroda and W. Mashiko, 2013: *CAS/JSC WGNE Res. Activ. Atmos. Oceanic Modelling,* **43**, 5.09-5.10.

Acknowledgements

This study was supported by MEXT Strategic Programs for Innovative Research (SPIRE), Field 3.

High-resolution COSMO-Ru1 model
and its application for the meteorological support
of Sochi-2014 Olympics and Paralympics

Marina Shatunova, Gdaly Rivin, Inna Rozinkina
Hydrometeorological Research Center of Russia
gbert@yandex.ru

A new version of COSMO model with grid spacing of 1.1 km named COSMO-Ru1 was developed for the weather forecasting during the Sochi Olympics and Paralympics in 2014 as a part of the Priority Project *CORSO* (cosmo-model.org/content/tasks/priorityProjects/corso/default.htm) of the COSMO consortium (www.cosmo-model.org). The main goal of this project was to demonstrate the capabilities of COSMO-based systems for short-range numerical weather prediction in winter conditions over mountainous terrain.The results of the CORSO project are summarized in the presentation (cosmo-model.org/content/tasks/achievements/docs/2014_CORSO.pdf)

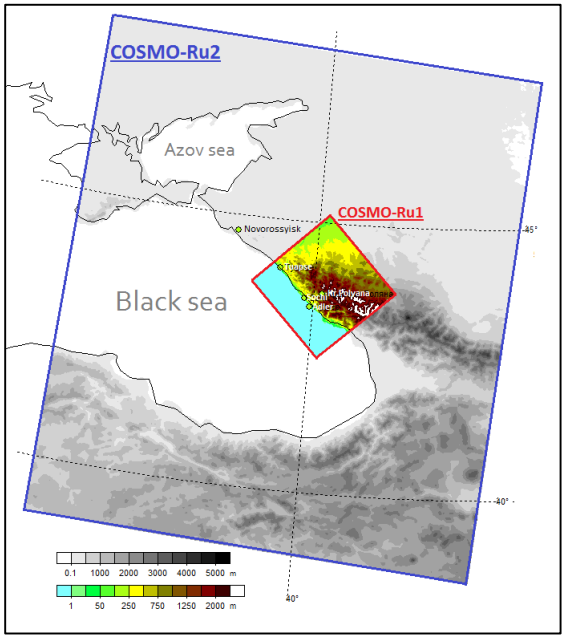

Fig. 1. COSMO-Ru1 and COSMO-Ru2 models domains and models orography.

COSMO-Ru1 model domain with dimension 210 x 210 km was nested into the greater domain of COSMO-Ru2 version with grid spacing of 2.2 km (Fig.1) used as a driving model. At the first step (Shatunova, Rivin, 2014), the impact of external parameters on the simulation results of the high resolution model for the region with complicated topography was examined. The influence of the model integration domain size and model orography on temperature and precipitation forecast was studied. Numerical experiments with model domain with grids of 100 x 100, 190 x 190 and 400 x 400 nodes were conducted. Domain 190 x 190 was considered optimal in terms of the ratio of computation time and accuracy of forecast.

The operational version of COSMO-Ru1 has a grid with 190 x 190 nodes and there are 50 vertical levels up to 22 km. The time step was set to five seconds to prevent possible failures of the run in case of strong convection. Such cases have been reported with the south-west wind carrying warm humid air from the Black Sea to the Caucasus Range during autumn and early winter.

Initially COSMO-Ru1 model was designed as a research version. Based on the verification and case studies results it was decided to run COSMO-Ru1 model in operational mode. For the period of Olympic and Paralympic games the model ran 4 times per day starting from the COSMO-Ru2 previous forecast (- 6 h). That was made in order to meet forecaster's requirements and to provide them with forecasts (model output) at 4 a.m. local time.

The model provided forecast charts for the whole model domain and for two "subdomains" where the fields of meteorological elements were presented in more detail – the coastal region and the mountain valley region. Complex charts "relative humidity & streamlines" and charts of streamlines within the valley were most popular among forecasters. Meteograms for several location were also provided.

COSMO-Ru1 model forecasts were verified using VERSUS software and some first results were presented by A. Bundel et al. (2014).

Before the Olympic games, during a so-call trial period, the weather monitoring network was extended in the Sochi region and a wide variety of observation data including profilers, radars, satellites and even web-cameras became available. This allowed to do not only standard verification procedures but to perform several case studies in order to understand the model behavior and to evaluate 1 km grid-spacing model advantages for weather forecasting in mountainous terrains against coarser-resolution models. Two low visibility case studies (Shatunova et al., 2015) demonstrate the capabilities of COSMO-Ru1 model very well. It is shown that the use of COSMO-Ru1 model output allowed to give a detailed forecast of visibility changes with a leadtime of 24 hours .

Bundel A. Yu., A.A. Kirsanov, A.V. Muraviev, G.S. Rivin, I.A. Rozinkina, D.V. Blinov, 2014: First verification results for COSMO-Ru mesoscale numerical weather forecasts issued for the Soch-2014 Olympics. Proceedings of Hydrometcenter of Russia, vol. 352, 37-54 pp. (*in Russian*).

Shatunova M.V., G.S. Rivin, 2014: High resolution model COSMO-Ru1SFO: influence of the external parameters on model output. Proceedings of Hydrometcenter of Russia, vol. 352, 150-167 pp. (*in Russian*).

Shatunova M.V., G.S. Rivin, I.A. Rozinkina, 2015: Visibility forecast for February 16-18, 2014 for the region of Sochi-2014 Olympics by means of high-resolution COSMO-Ru1 model. Meteorology and Hydrology, № 8 (*in press*).